Vertical Gradient in Regional Vascular Resistance and Pre to Post Capillary Resistance Ratios in the Dog Lung

J.C. Parker, R.E. Parker, D.N. Granger, A.E. Taylor

Department of Physiology, University of South Alabama, Mobile, Alabame

Summary

The ratios of pre-capillary (R_a) and post-capillary (R_v) resistances to total vascular resistance (R_T) were measured at different vertical distances in the lungs of supine dogs. Capillary pressures were estimated as the algebraic sum of the alveolar absorption pressure for Tyrode's solution and the plasma colloid osmotic pressure. Segmental resistance fractions (R_a/R_T, R_v/R_T) were calculated using the pressure drops between arterial, capillary, and venous pressures at each vertical distance within the lung. In a second group of animals, total vascular resistance was calculated at each lung level using regional blood flow as measured by radiolabelled microspheres and the corresponding regional vascular pressures. The total vascular resistance was lowest in Zone III portions of the lung, but R_a/R_T and R_v/R_T were constant throughout this zone (n = 22) averaging .63 ± .02 (SEM) and .37 ± .02 (SEM, respectively, resulting in R_a/R_v of 1.70). Total vascular resistance increased markedly in Zone II portions of the lung, but the relative contribution of R_a/R_T decreased from .62 ± .07 (SEM) to .45 ± .05 (SEM). Thus R_a/R_v decreased from 1.70 to .82 in Zone II. The absolute values of pre- and post-capillary resistances were lowest in Zone III but post-capillary resistance increased to a greater degree than pre-capillary resistance up Zone II.

Introduction

Recently there has been a renewed interest in the forces that regulate fluid movement across the pulmonary microcirculation. Obviously, the major force that drives the fluid, which ultimately forms pulmonary lymph, into the interstitial spaces is the capillary pressure, and attempts have been made to estimate segmental vascular resistances so that capillary pressures may be calculated in intact lungs using vascular inflow and outflow pressures (1–6). Only in a few laboratories has capillary

pressure been measured directly and these estimations were conducted in either open-chested dogs or, isolated perfused lungs (7–9).

An accurate estimate of capillary pressure is essential because many investigators are currently monitoring pulmonary artery pressure, left atrial pressure, and the flow rate and protein concentration of pulmonary lymph in intact animals in order to describe the fluid and protein movement across the filtering vessels in the lung (10). When constructing a fluid balance equation with this data, the filtration pressure at the capillaries is calculated from the measured vascular pressures and the post-capillary resistance obtained by *Gaar* et al. (8) which was evaluated in non-ventilated, isolated, perfused dog lungs. However, introduction of certain drugs, increased alveolar pressure, and increased left atrial pressure will certainly alter pre- and post-capillary resistances, and the vascular reactivity of intact lungs may differ considerably from that observed in isolated lung preparations.

In addition, it is well known that capillary pressures will differ at different lung levels in normal lungs, with higher pressures being present in the more dependent regions of the lung. Estimates of total transvascular fluid filtration from composite lymph samples will be in error to the extent that the gradient in capillary pressure causes non-homogeneity in the regional lymph composition and flow rate between the top and bottom of the lung. While pressure in the filtering vessels may be expected to vary along a hydrostatic gradient over most of the vertical division of the lung, the unique property of the lung having an airspace immediately adjacent to the pulmonary capillary network leads to interaction

between the pressure of alveolar air (P_{alv}) and the pulmonary arterial (P_a) and venous pressures (P_v). In fact, the lung may be divided into blood flow zones based on the relationship of these three pressures, such that in zone I ($P_{alv} > P_a > P_v$) and zone II ($P_a > P_{alv} > P_v$), the regional blood flow and microvascular pressures are largely controlled by alveolar pressure, whereas in zone III ($P_a > P_v > P_{alv}$) the filtration pressures and blood flow are largely independent of alveolar pressures. From these considerations, it is evident that a complex set of conditions determinine the capillary filtration pressure at each vertical region of the lung and we have no means of directly measuring capillary pressure in the lungs of intact animals or of estimating the regional pre- and post-capillary resistance in order to calculate capillary pressure from arterial and venous pressures. Yet, the capillary pressure must be known before the forces which determine lymph flow and fluid balance can be adequately described.

The following study presents a method for estimating capillary pressures based on measurements of alveolar fluid absorptive pressures. Although the method must incorporate many assumptions, it does represent a rational approach for estimating how microvascular pressures change in lungs of intact animals when subjected to various experimental manipulations. The present study relates microvascular pressures to the inflow and outflow pressures at various lung levels and indicates that the pre- and post-capillary resistances are relatively constant throughout zone III and they are similar in magnitude to published measurements made in isolated dog lungs. The method outlined in this paper provides a new approach for assessing capillary pressures in intact, spontaneously breathing animals without the necessity of assuming a constant relationship between pre- and post-capillary resistance.

Methods

1. Capillary Pressure Measurement

The basic method used to obtain absorptive pressure for alveolar fluid has been previously described in detail (11). Briefly, the animals

(14.5–22.3 kg) were anesthetized with sodium pentobarbital (30 mg/kg) and then ventilated with pure oxygen for two minutes using a Harvard respirator. One or two # 5 Swan-Ganz catheters were then inserted under fluoroscopic control and the position of the catheter tips measured with respect to a pulmonary artery catheter. To do this, a large three-prong wooden caliper with radio-opaque tips was superimposed on ends of the catheters. Immediately after lodging a catheter into the bronchus, the balloon was inflated and .5–1.5 ml of fluid was flushed into the alveolar segment. Subsequent absorption of residual oxygen from the alveolar spaces resulted in a completely fluid-filled segment.

A Statham pressure transducer was zeroed at the level of the bronchial catheter tip, and the system was closed to the atmosphere. The pressure in each occluded alveolar segment was allowed to equilibrate over a 30 to 40 minute period, when the dog was placed in the supine position. The pressures recorded in the alveolar fluid were invariably more negative in upper than lower portions of lung. An additional Swan-Ganz catheter was placed in the pulmonary artery and wedged to estimate left atrial pressure. Plasma colloid osmotic pressure was measured using a membrane type colloid osmometer (12).

Using basic fluid flux equations for both the alveolar epithelium and capillary endothelial membranes, an equation relating alveolar fluid pressure (P_{af}) to interstitial fluid pressure (P_i), interstitial colloid osmotic pressure (π_i), and the osmotic reflection coefficient of the alveolar epithelium (σ_a), was derived for steady-state conditions in the Tyrode's filled segments (11). The balance of pressures across the alveolar membrane is:

$$P_{af} = P_i - \sigma_a \pi_i \qquad (1)$$

Although interstitial forces determine the fluid absorptive pressure in the alveolar compartment, the interstitial forces are ultimately determined by the capillary hydrostatic pressure (P_c), plasma colloid osmotic pressure (π_c), the osmotic reflection coefficient of the capillaries (σ_c), the capillary fluid filtration coefficient (K_{fc}), and the lymph flow rate (J_v)

The equation for fluid flux across the capillary membrane is:

$$J_{vc} = K_{fc} (P_c - \sigma_c \pi_c + \sigma_c \pi_i - P_i) \qquad (2)$$

By solving equation (1) for P_i, and substitution into equation (2), the resulting equation can be solved for capillary pressure to yield the following equation:

$$P_c = P_{af} + \sigma_c \pi_c + (\sigma_a - \sigma_c) \pi_i + \Delta P_c \qquad (3)$$

The net pressure imbalance across the capillary endothelium resulting from lymph flow is represented by ΔP_c (which is equal to J_{vc}/K_{fc}). If the contribution of the last two terms is small, the pulmonary capillary pressure, P_c', may be estimated in a closed chested animal using only the alveolar fluid absorptive pressure and plasma colloid osmotic pressure. This assumes an effective colloid osmotic pressure equivalent to that measured on the osmometer, or an osmotic reflection coefficient near unity for the capillary membrane; and yields the following equation:

$$P_c' = \pi_c + P_{af} \qquad (4)$$

A similar relationship was used by *Agostoni* and *Piiper* (7) to estimate pulmonary capillary pressure by using the fluid absorptive pressure at the pleural surface and the plasma colloid osmotic pressure.

Since the permeability of the alveolar epithelium and the regional interstitial protein concentration of the fluid filled segments was not measured, we must consider the conditions for which the last two terms in equation 3 could be neglected without causing a significant error when capillary pressure was calculated by equation 4.

(1) $\sigma_a \cong 0$, $\sigma_c \cong 1$, $\pi_i < \pi_c$, and $\Delta P_c \cong 0$. For this case, the alveolar epithelium would be disrupted allowing bulk flow into the interstitium, and the estimate of P_{af} would be equivalent to tissue pressure (P_i).

(2) $\sigma_a \cong \sigma_c \cong 1$, and $\Delta P_c \cong 0$. If the alveolar epithelium and capillary endothelium were relatively impermeable to proteins, then the total absorptive force of the interstitium ($P_i - \pi_i$) would be measured by the alveolar fluid absorptive pressure. If ΔP_c is also small, then there is no problem with estimating capillary pressure from equation 4.

(3) $(\sigma_a - \sigma_c) \pi_i + \Delta P_c = 0$. If the alveolar membrane was partially disrupted such that σ_a was slightly lower than σ_c then ΔP_c could equal this term and allow P_c to be estimated by equation 4.

Conditions 1 and 3 would require a change in the normal permeability of the alveolar epithelium, which is generally considered to be a tight epithelium severely restricting the passage of proteins (13). However, several recent studies have indicated that when only small pressure gradients are imposed across the epithelium of fluid filled lungs then proteins easily pass across this barrier (14–15). In addition, since ΔP_c estimated for dog lungs is only .5–1 mm Hg at normal pulmonary vascular pressures, then the lymphatic factor should be small (16). Although any of these three conditions are possible, condition 2 is the most physiologically appealing because both membranes should have a low permeability to proteins unless the alveolar membrane is disrupted.

2. Regional Pulmonary Blood Flow

Mongrel dogs weighing between 15.2 and 24.6 kg were anesthetized as previously described. The regional blood flows were measured with the animals in the supine position because supine dogs have an ample lung height (15–20 cm) in which to study gravity dependent gradients in flow and pressure, and the animals can maintain normal vascular pressures and cardiac output over several hours. The animals were prepared by passing a # 5 Swan-Ganz catheter via the right external jugular into the pulmonary artery. In this way, pulmonary artery pressure was continuously monitored and periodic pulmonary wedge pressures were obtained. The dogs were injected with 1000 units/kg sodium heparin for anticoagulation and allowed to breathe spontaneously. A large bore catheter was passed through the left external jugular into the right atrium, and connected to another catheter leading to a femoral artery. Blood continuously

flowed at approximately 150 to 200 ml/min from femoral artery to right atrium through this catheter which had a rubber port for injection of the microspheres used to measure regional blood flow. A bolus of plastic microspheres (3M Company, St. Paul, Minnesota 55101) with a mean diameter of 15 microns and labelled with either Sr^{85} or Ce^{141} was injected into the rubber port of the flowing catheter. Blood was withdrawn at a constant rate from the pulmonary artery catheter for two minutes after the injection to sample the microsphere bolus as it passed into the lung.

After the microsphere injection, the animals were exsanguinated. Then the lungs were removed and inflated with a continuous 25 cm H_2O airway pressure and placed into a freezer. The next day the frozen lungs were cut into two centimeter slices on planes perpendicular to the axis of gravity for the supine dog. Four to six samples of each lung slice were taken with a 1 cm diameter cork borer. These frozen lung samples were placed in counting tubes and counted on a Packard Model 3000 three-channel gamma counter. When both isotopes were used in the same animal, corrections were made for overlap between the gamma energy spectrums.

The regional blood flow (RBF) in each lung sample was calculated on a per gram wet weight basis from the pump withdrawal rate (WD), the total counts per minute in the pulmonary artery blood withdrawn (CB), and the counts per minute in the tissue sample (CT), by the expression:

$$RBF = (WD \times CT)/CB \qquad (5)$$

These blood flows together with simultaneously measured pulmonary artery and venous pressures were used to estimate the regional vascular resistance.

Results

Table 1 summarizes the data obtained in 21 dogs. The fractions of the total vascular resistance (R_t), upstream (R_a/R_t) and downstream (R_v/R_t) from the hypothetical filtration midpoint, were calculated at each vertical distance up the lung from the capillary pressures obtained using equation 4 and the arterial (P_{pa}) and wedge (P_w) pressures in each experiment corrected for vertical distance up the lung, using the following relationships:

$$R_a/R_t = (P_{pa} - P_c')/(P_{pa} - P_w) \qquad (6)$$

and

$$R_v/R_t = (P_c' - P_w)/(P_{pa} - P_w) \qquad (7)$$

Tab. 1 Summary of the vascular pressures and segmental vascular resistances at different vertical distances in the lung

V.D. cm	n	Zone	R_a/R_t	R_v/R_t	R_a/R_v	P_{pa}	P_w	P_{alv}	P_c^2	P_c^3
17	3	II	.45 ± .05[4]	.55 ± .05[4]	.82	17.0	-5.0	0	7.1	5.3
15	3	II	.53 ± .07	.47 ± .07	1.13	19.0	-3.0	0	7.34	6.6
13	6	II	.58 ± .03	.42 ± .03	1.38	21.0	-1.0	0	8.24	8.0
11	3	III	.62 ± .07	.38 ± .07	1.63	23.0	1.0	0	9.36	9.8
9	4	III	.65 ± .04	.35 ± .04	1.86	25.0	3.0	0	10.70	11.8
7	3	III	.63 ± .03	.37 ± .02	1.70	27.0	5.0	0	13.14	13.8
5	4	III	.63 ± .06	.37 ± .06	1.70	29.0	7.0	0	15.14	15.8
3	3	III	.64 ± .02	.36 ± .02	1.78	31.0	9.0	0	16.92	17.8
1	3	III	.63 ± .05	.37 ± .05	1.70	33.0	11.0	0	19.14	19.8

1. V.D. = vertical distance up the lung. All pressures are tabulated as cm H_2O, and resistances are shown as means ± standard error.
2. $P_c = (R_v/R_t) (P_{pa}-P_w) + P_w$
3. $P_c = .4(P_{pa}-P_w) + P_w$ for Zone III, and $P_c = P_{pa} - [.6 + .4(P_t-P_{pa})/P_t] (P_{pa}-P_{alv})$ for Zone II, where P_t is the pulmonary artery pressure at the transition between Zones II and III.
4. Statistically different (p < .05) from Zone III fractional resistances.

All resistances for each 2 cm vertical distance segment were averaged to obtain a mean ± standard error for that vertical distance.

When all 22 determinations in the lower six segments were averaged together, a relative pre-capillary resistance of .63 ± .02 (SEM) was obtained, indicating a constant fraction of pre- and post-capillary resistance in Zone III lung, i.e., where arterial and venous pressure exceed alveolar pressure. However, the relative pre-capillary resistance decreased significantly (p < .05) from .62 ± .07 (SEM) to .45 ± .05 (SEM) up Zone II, i.e., where alveolar pressure exceeds venous pressure. The pre/post capillary resistance ratios (R_a/R_v) remained constant throughout Zone III averaging 1.70, but the ratio decreased to .82 in the uppermost region of Zone II.

The mean pulmonary artery pressure of 25.0 ± .73 (SEM) cm H_2O and pulmonary wedge pressure of 5.98 ± .34 (SEM) cm H_2O were used for estimates of regional pulmonary artery (P_{pa}) and venous (P_w) pressures at each vertical distance in the hypothetical average lung shown in Table 1, assuming a hydrostatic gradient of 1 cm H_2O/cm vertical distance. From these regional inflow and outflow pressures and the regional post-capillary resistance, capillary pressures (P_c^2) were calculated for each vertical segment by the following equation:

$$P_c^2 = (R_v/R_t)/(P_a - P_w) + P_w \qquad (8)$$

For comparison, another set of regional capillary pressures (P_c^3) was also calculated from the same regional pulmonary artery and venous pressures using the formula for Zone III capillary pressure derived empirically by Gaar et al. (7):

$$P_c^3 = .4 (P_{pa} - P_w) + P_w \qquad (9)$$

and the following capillary pressure equation for Zone II derived by Staub (10):

$$P_c^3 = P_{pa} - [.6 + .4 (P_t - P_{pa})/P_t] (P_{pa} - P_{alv}) \qquad (10)$$

where P_t is the pulmonary artery pressure at the transition point between Zone II and III, and P_{alv} is alveolar pressure.
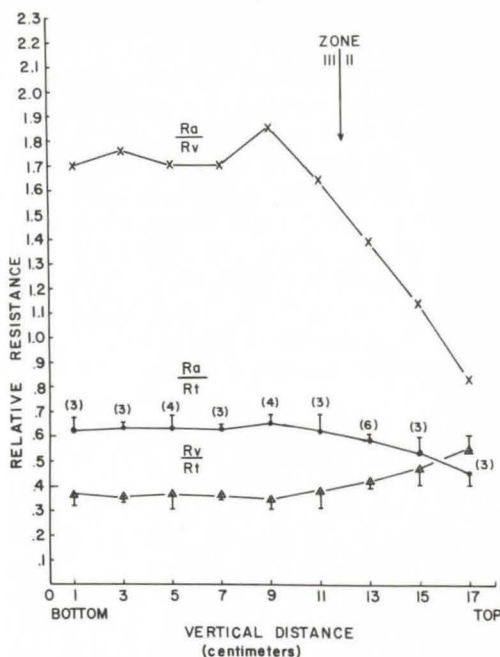

Fig. 1 The relationship between fractional pre-capillary (R_a/R_t), post-capillary resistance (R_v/R_t) and the pre/post-capillary resistance ratios (R_a/R_v) at different lung levels. The data points represent the means of pre- and post-capillary resistances calculated from individual experimental values for each 2 cm vertical region of lung. R_a/R_v's were calculated using the mean values for R_a/R_t and R_v/R_t

Figure 1 is a graph showing R_a/R_t, R_v/R_t, and R_a/R_v as a function of vertical distance up the lungs. This figure illustrates that R_a/R_t, R_v/R_t, and R_a/R_v were constant throughout Zone III, but all three parameters changed dramatically in Zone II. However, the Zone II R_a/R_t and R_v/R_t ratios were only statistically different (p < .05) from the average for all the Zone III ratios at 17 cm vertical distance up the lung when the groups were compared by a grouped "t" test.

The relationship between the capillary pressure (P_c^2) calculated from equation 10, and vertical height is shown in Figure 2. Also shown in the graph are the venous and arterial pressures from which the capillary pressures were calculated. The pulmonary venous pressure intersects alveolar pressure, assumed to equal atmospheric pressure in the spontaneously breathing dogs,
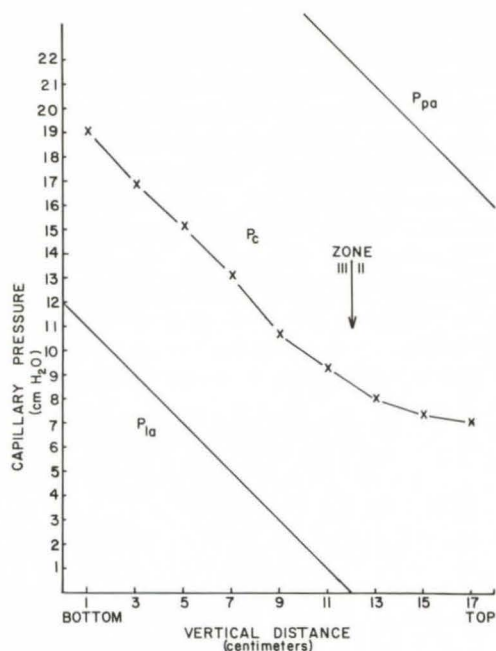
Fig. 2 Plot of the relationship between capillary pressure (P$_c$) and vertical distance. Capillary pressures were calculated from a hydrostatic distribution of left atrial (P$_w$) and pulmonary artery (P$_{pa}$) pressures using the mean post-capillary resistance at each vertical level
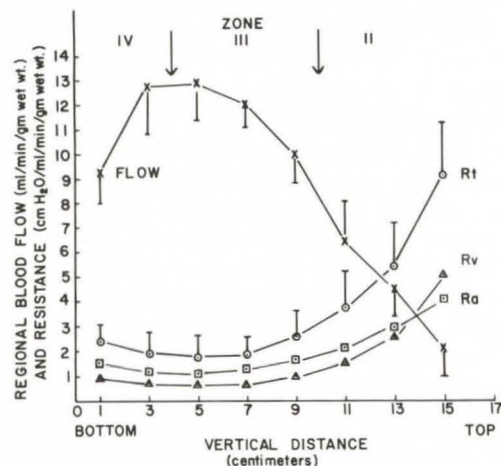

Fig. 3 A plot demonstrating the relationship between regional blood flow, total vascular resistance (R$_t$), pre-capillary (R$_a$), and post-capillary resistances (R$_v$) from the bottom to the top of the lung. Data points represent means ± SEM and the arrows indicate the transition level between zones

at the transition point between Zones III and II. Capillary pressure in the average lung demonstrated a hydrostatic gradient of approximately 1 cm H_2O/cm vertical distance in the lower lung, but the gradient decreases in Zone II of the upper lung. However, the capillary pressure in Zone II must approach alveolar or pulmonary arterial pressure at some point before regional pulmonary arterial pressure equals alveolar pressure, i.e., the transition point between Zones II and I.

Figure 3 indicates how both regional blood flow and vascular resistance change at different vertical distances up the lung in supine dogs. The flow curve is a composite of six microsphere determinations in four dogs and each mean consists of 30 tissue samples. The regional blood flow increased down the lung except at the very base where regional blood flow decreased in every experiment. The blood flow zones within the lung were defined according to West et al. (17). That is, Zone I is the area where P$_{alv}$ > P$_{pa}$ > P$_{la}$ and no blood flow is present. However, no areas of absent flow were found in any of these experiments. Zone II of the lung was defined as that portion of lung where venous pressure is less than alveolar air pressure (P$_{pa}$ > P$_{alv}$ > P$_{la}$), and Zone III as the region where both arterial and venous pressure exceed alveolar pressure (P$_{pa}$ > P$_{alv}$ > P$_{la}$). In addition, Zone IV has been designated as the lower portion of Zone III lung where regional perfusion was reduced.

The regional vascular resistance (R$_t$) was calculated from the regional pulmonary artery (P$_{pa}$), and venous (P$_w$) pressures and regional blood flow ($\dot{Q}_r$) by the equation:

$$R_t = (P_{pa} - P_w)/\dot{Q}_r \tag{11}$$

The total regional resistance was markedly increased in the upper lung as opposed to the mid-regions of lung. A region of slightly increased resistance was also consistently found in the lowermost portion of the lung (Zone IV). The regional pre- (R$_a$/R$_t$) and post- (R$_v$/R$_t$) capillary resistance fractions shown in Table 1 were multiplied by the regional vascular resistances (R$_t$) to obtain the pre-capillary (R$_a$) and post-capillary resistance (R$_v$) shown in the graph.

Tab. 2 A summary of pre- (R_a) and post- (R_v) capillary resistances measured by various methods and expressed as a fraction of total vascular resistance

R_a	R_v	R_a/R_v	Method	Reference
.40	.60	.67	fluid absorption	*Agostoni* et al. (1962)
.56	.44	1.27	isogravimetric	*Gaar* et al. (1967)
.63	.37	1.70	low viscosity bolus	*Brody* et al. (1963)
.69	.31	2.22	low viscosity bolus	*Dawson* et al. (1977)
.71	.29	2.45	Starling resistor model	*Gilbert* et al. (1972)
.62	.38	1.63	segmental pressure drop	*Kuramoto* and *Rodbard* (1962)
.52	.48	1.08	isofiltration	*Gabel* and *Drake* (1978)
.63	.37	1.70	fluid absorption	present study
.60	.40	1.50	mean of column	

Thus, the pre- and post-capillary resistances were relatively constant throughout Zone III, but both pre- and post-capillary resistance increased in Zone II even through the fractional pre-capillary resistance was reduced. The major portion of the increased Zone II resistance was attributed to a large increase in post-capillary resistance.

Discussion

Table 2 summarizes the fractions of total resistance found upstream and downstream from the functional capillary midpoint by various techniques. There is good agreement between the vascular resistances found in Zone III lungs using a variety of experimental methods. Many of these studies appear to validate the formula (Equation 10) empirically derived from isogravimetric capillary pressures in isolated dog lungs by *Gaar* et al. (8). *Agostoni* and *Piiper* (7) first estimated capillary pressure from the absorption pressure for Tyrode's at the pleural surface and the plasma colloid osmotic pressure. The pre/post capillary resistance ratio was then calculated from the capillary pressure and vascular inflow and outflow pressures. *Gabel* and *Drake* (9) used an isofiltration technique, whereby arterial and venous pressure are converged in steps, while keeping the lung lobe filtering at a constant rate. Two or more isofiltration vascular pressure states were required to solve for the relative post-capillary resistance. *Brody* et al. (1), and later *Dawson* et al. (2) measured the time-course of the pressure drop in the pulmonary circulation as a low viscosity bolus of saline passed through

an isolated lung preparation perfused at a constant rate. Using Poiseuille equation, the major site of vascular resistance could be identified. *Gilbert* et al. (4) used the pressure-flow relationships inherent in a Starling resistor to calculate pre- and post-capillary resistances in the lung. These investigators assumed that Zone II resistance represented only the pre-capillary resistance, whereas Zone III vascular resistance represented the sum of both pre-capillary by total vascular resistance, and a relative pre-capillary resistance was obtained. Still another approach was used by *Kuramoto* and *Rodbard* (5), who wedged a small catheter into the small pulmonary veins from the downstream side and calculated a post-capillary resistance from the pressure difference between the small wedged veins and the left atrium. They also found that a major portion of total vascular resistance was upstream from the small veins. In the present study, we found the pre/post capillary resistance ratio was very constant throughout Zone III, with a mean value of 1.70. The relative pre-capillary and post-capillary resistances averaged .63 and .37 respectively. An average of the resistance obtained by all of the methods in Table 2 indicate that the total vascular resistance was distributed approximately sixty percent upstream and forty percent downstream from some capillary midpoint. It is apparent that the measurements for Zone III resistances obtained in the present study are in agreement with results obtained by a variety of other methods in open-chest and isolated lung preparations.

In contrast to the agreement between methods as to the distribution of segmental vascular resistance in Zone III, there is disagreement as to the predominant site of vascular resistance caused by the "waterfall" or "sluice" effect found in Zone II regions of lung. Some investigators have found a predominance of upstream resistance in Zone II lungs. *DeBono* and *Caro* (18) concluded that the downstream resistance was determined by the alveolar pressure under Zone II conditions, but that a major portion of the vascular resistance remained in the arterioles. *Glazier* et al. (19) described the histologic appearance of the alveolar septal vessels in frozen lung sections, and concluded there was a significant pre-capillary resistance in Zone II.

Our results also indicate an increase in pre-capillary resistance in Zone II regions, but the predominant increase in vascular resistance was found to be post-capillary. Even though fractional pre-capillary resistance decreased from .62 to .45 up Zone II, the corresponding increase in vascular resistance was such that pre-capillary resistance increased in absolute terms. However, post-capillary resistance increased in both relative and absolute terms up Zone II. A similar observation was reported by *Dawson* et al. (20), using the low viscosity bolus technique, who found that the pre/post capillary resistance ratio decreased from 2.20 to .75 as transpulmonary pressure was increased in steps from 0 to 16 cm H_2O, with left atrial pressure set at 0 cm H_2O. This decrease indicates that there was an increased proportion of the total vascular resistance downstream from the capillary midpoint as the alveolar pressure progressively increased above the venous pressure. An increasing post-capillary resistance up Zone II suggests a downstream collapse point in the vessels which moves towards the arterial end of the microvessels.

Other investigators have found a large fraction of the resistance post-capillary in Zone II conditions. *Fowler* et al. (3) perfused isolated lungs both in forward and reverse directions in zone II conditions. They observed that 50% of the total vascular resistance occurred in the alveolar vessels, and that the down-stream collapse point accounted for the majority of the total vascular resistance. *McDonal* and *Butler* (6) used a similar Starling resistor lung model, but used both air and liquid filled lungs The alveolar vessels contribution was found to increase from 35% to 80% of total vascular resistance when alveolar pressure exceeded venous pressure, but the exact site of the compression or sluice point could not be identified. Based on a sheet flow analysis of the alveolar capillary network, *Fung* and *Sobin* (21) predicted a major pressure drop at the downstream end of the capillary bed in zone II lungs which is compatible with the basic pressure-flow characteristics of a Starling resistor (22).

The capillary pressures calculated from our data for zone II are similar in magnitude to the pressures calculated using equation 10 derived by *Staub* (10). However, the coefficients of this equation may be modified slightly to achieve a more exact fit of the experimental data such that:

$$P_c = P_{pa} - [.54 + .42 (P_t - P_{pa})] (P_{pa} - P_{alv}) \quad (12)$$

The zone II capillary pressures described by this equation approach the intersection of pulmonary artery and alveolar pressures (zone I/II transition) in a curvilinear fashion such that the capillary pressures are higher at every vertical level than would be calculated by assuming a constant post capillary resistance, because capillary pressure exceeds alveolar pressure until $P_{pa} = P_{alv}$. Although only the fractional post capillary resistance increased up zone II, both pre- and post-capillary resistances were increased in absolute resistance terms. The increasing pre-capillary resistance suggests derecruitment of capillary networks up the lung because of the lower perfusion pressures (23), whereas the increasing post-capillary resistance is compatible with a downstream collapse point shich is the major site of vascular resistance in zone II (24).

The effect of this vertical gradient of capillary pressure on regional lymph flow is unknown, because there are no available data relative to regional lymph flows under different zonal conditions in the lung. Although there are

clearly different hydrostatic pressures in the filtering vessels, the net filtration pressure for lymph flow is determined by the sum of forces across the endothelial membrane as shown in equation 2. If the interstitial hydrostatic pressure is invariant between top and bottom of the lung (25), then regional lymph flow will increase in proportion to the increase in capillary pressure down the lung. In addition, there may be a larger regional interstitial volume and a smaller interstitial colloid osmotic pressure towards the bottom of the lung (10). However, fluid within the interstitial matrix is continuous and unbound (26) so the gradient in interstitial fluid pressure would tend to approach a hydrostatic gradient at equilibrium (27, 28). To the extent that the vertical gradient in interstitial fluid pressure approaches a hydrostatic gradient there would be a more equal net filtration pressure across the capillary membrane at different vertical levels with a more homogeneous regional lymph flow and interstitial colloid osmotic pressure between top and bottom of the lung. In fact, preliminary experimental data have demonstrated a vertical gradient in interstitial fluid pressure (29) and no significant difference in regional lymph protein concentration at different lung levels (30). Further measurements of regional pulmonary lymph flows and protein concentrations are required before the true significance of the vertical gradient in capillary pressure for transcapillary fluid filtration can be established.

Acknowledgements

References

1 Brody, J.S., E.J. Stemmler, A.B. DuBois: Longitudinal distribution of vascular resistance in the pulmonary arteries, capillaries, and veins. J. Clin. Invest. 47 (1968) 783

2 Dawson, C.A., R.L. Jones, L.H. Hamilton: Hemodynamic responses of isolated cat lungs during forward and retrograde perfusion. J. Appl. Physiol. 35 (1973) 95–102

3 Fowler, K.T., J.B. West, M.C.F. Pain: Pressure-flow characteristics of horizontal lung preparations of minimal height. Respiration Physiol. 1 (1966) 88–98

4 Gilbert, R.D., J.R. Hessler, D.V. Eitzman, S. Cassin: Site pulmonary vascular resistance in fetal goats. J. Appl. Physiol. 32 (1972) 47–53

5 Kuramoto, K., S. Rodbard: Effects of blood flow and left atrial pressure on pulmonary venous resistance. Circ. Res. 11 (1962) 240–246

6 McDonald, I., J. Butler: Distribution of vascular resistances in the isolated perfused dog lung. J. Appl. Physiol. 23 (1967) 463–474

7 Agostoni, E., J. Piiper: Capillary pressure and distribution of vascular resistance in isolated lung. Am. J. Physiol. 202 (1962) 1033

8 Gaar, K.A., Jr., A.E. Taylor, L.J. Owens, A.C. Guyton: Pulmonary capillary pressure and filtration coefficient in the isolated perfused lung. Am. J. Physiol. 213 (4) (1967) 910–914

9 Gabel, J.C., R.E. Drake: Pulmonary microvascular pressure in intact dogs. Microvasc. Res. 15 (1978) 263

10 Staub, N.C.: Pulmonary edema. Physiol. Rev. 54 (1974) 678

11 Parker, J.C., A.C. Guyton, A.E. Taylor: Pulmonary interstitial and capillary pressures estimated from intra-alveolar fluid pressures. J. Appl. Physiol. 44 (2) (1978) 267–276

12 Prather, J.W., K.A. Gaar, Jr., A.C. Guyton: Direct continuous recording of plasma colloid osmotic pressure of whole blood. J. Appl. Physiol. 24 (1968) 602–605

13 Taylor, A.E., K.A. Gaar, Jr.: Extimation of equivalent pore radii of pulmonary capillary and alveolar membranes. Amer. J. Physiol. 218 (1970) 1133–1140

14 Gee, M.H., N.C. Staub: Role of bulk fluid flow in protein permeability of the dog lung alveolar membrane. J. Appl. Physiol.: Respirat. Environ. Exercise Physiol. 42 (2) (1977) 144–149

15 Egan, E.A., R.M. Nelson, R.E. Olver: Lung inflation and alveolar permeability to non-electrolytes in the adult sheep in vivo. J. Physiol. London. 260 (1976) 409–424

16 Taylor, A.E., R.E. Drake: Fluid and protein movement across the pulmonary microcirculation. In: Lung Water and Solute Exchange (Ed.) N.C. Staub. Marcel Dekker, Inc., New York (1978)

17 West, J.B., C.T. Dollery, A. Naimark: Distribution of blood flow in isolated lung; relation to vascular and alveolar pressures. J. Appl. Physiol. 19 (1964) 713

18 DeBono, E.F., C.G. Caro: Effect of lung-inflation pressure on pulmonary blood pressure and flow. Am. J. Physiol. 205 (1963) 1178–1186

19 Glazier, J.B., J.M.B. Hughes, J.E. Maloney, J.B. West: Measurements of capillary dimensions and blood volume in rapidly frozen lungs. J. Appl. Physiol. 26 (1) (1969) 65–76

20 *Dawson, C.A., D.J. Grimm, J.H. Linehan:* Effects of lung inflation on longitudinal distribution of pulmonary vascular resistance. J. Appl. Physiol. 43 (6) (1977) 1089–1092

21 *Fung, Y.C., S.S. Sobin:* Theory of sheet flow in lung alveoli. J. Appl. Physiol. 26 (1969) 472

22 *Permutt, S., B. Bromberger-Barnea, H.N. Bane:* Alveolar pressure, pulmonary venous pressure, and the vascular waterfall. Med. Thorac. 19 (1962) 239–260

23 *West, J.B., A.M. Schneider, M.M. Mitchell:* Recruitment in networks of pulmonary capillaries. J. Appl. Physiol. 39 (1975) 976

24 *Permutt, S., R.L. Riley:* Hemodynamics of collapsible vessels with tone: The vascular waterfall. J. Appl. Physiol. 18 (1963) 924–932

25 *Blake, L.H., N.C. Staub:* Pulmonary vascular transport in sheep. A Mathematical model. Microvascular Research 12 (1976) 197–220

26 *Compter, W.D., T.C. Laurent:* Physiologic function of connective tissue polysaccharides. Physiol. Revs. 58 (1978) 255–315

27 *Scholander, P.F.:* State of water in osmotic processes. Microvasc. Res. 3 (1971) 215–232

28 *Hughes, J.M.B.:* Pulmonary interstitial pressure. Bull. Physiopath. resp. 7 (1971) 1095–1123

29 *Parker, J.C., R.E. Parker, D.N. Granger, A.E. Taylor:* Vertical gradient in pulmonary interstitial fluid pressure. The Physiologist 21 (1978) 89

30 *Molstad, L.S., A.E. Taylor:* Effects of hydrostatic height on pulmonary lymph protein concentration. Microvasc. Res. 11 (1976) 124

Dr. James C. Parker, Department of Physiology, University of South Alabama, Mobile, Alabama 36688